

SPATIALLY HETEROGENEOUS DYNAMICS IN SUPERCOOLED LIQUIDS

M. D. Ediger

*Department of Chemistry, University of Wisconsin-Madison, Madison, Wisconsin 53706;
e-mail: ediger@chem.wisc.edu*

Key Words glass-forming liquid, non-exponential relaxation, diffusion, reorientation, cooperativity

■ **Abstract** Although it has long been recognized that dynamics in supercooled liquids might be spatially heterogeneous, only in the past few years has clear evidence emerged to support this view. As a liquid is cooled far below its melting point, dynamics in some regions of the sample can be orders of magnitude faster than dynamics in other regions only a few nanometers away. In this review, the experimental work that characterizes this heterogeneity is described. In particular, the following questions are addressed: How large are the heterogeneities? How long do they last? How much do dynamics vary between the fastest and slowest regions? Why do these heterogeneities arise? The answers to these questions influence practical applications of glass-forming materials, including polymers, metallic glasses, and pharmaceuticals.

INTRODUCTION

Most scientists are inclined to think of single-component liquids as being homogeneous. And why not? Many important properties can be explained by modeling a liquid as a homogeneous continuum. For example, in a typical physical chemistry textbook, viscosity, diffusion, ionic mobility, and the rates of chemical reactions are all described on this basis. As explained below, supercooled liquids are different than “ordinary” liquids in this regard. As a liquid is cooled below its melting point, dynamics slow dramatically, typically by more than 10 orders of magnitude before the transition to a glass occurs. A qualitative change in the character of molecular motion occurs with this slowing of dynamics. Near the glass transition, dynamics in one region of a supercooled liquid can be orders of magnitude faster than dynamics in another region only a few nanometers away. This heterogeneity in dynamics has important consequences for understanding transport properties and the kinetics of chemical reactions in such materials. It may also be a critical observation for understanding why dynamics slow so precipitously as the glass transition approaches.

In this review article, I present the evidence that indicates the existence of spatially heterogeneous dynamics in supercooled liquids and attempt to answer the following questions: How large are the heterogeneities? How long do they last? How much do dynamics vary between the fastest and slowest regions? Where do these heterogeneities come from? I begin with a brief introduction to supercooled liquids, as this sets the context for this review. Readers interested in different perspectives on spatially heterogeneous dynamics in supercooled liquids should consult reviews by Sillescu (1) and Bohmer (2). Other recent reviews, which collectively take a broader view of supercooled liquids and glasses, are also recommended (3–10a).

Overview of Thermodynamics and Dynamics of Supercooled Liquids

Figure 1a shows the specific volume V_{sp} as a function of temperature for a typical liquid. On cooling from high temperatures, a liquid may crystallize at T_m . A liquid that manages to pass T_m without crystallizing is called a supercooled liquid. As a supercooled liquid is cooled to lower temperatures, its density and viscosity

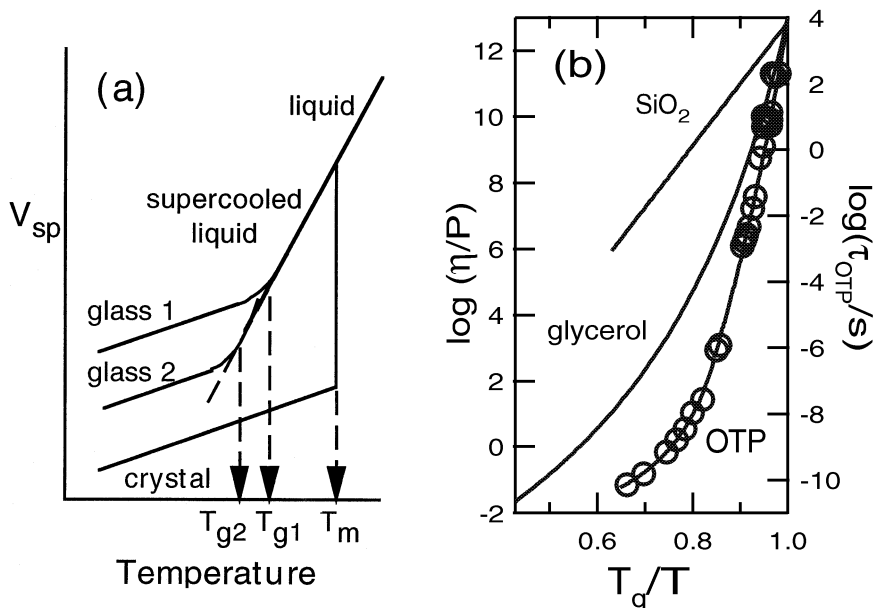


Figure 1 Thermodynamic (a) and dynamic (b) properties of supercooled liquids. (Solid lines) Viscosity of three liquids; (open circles) nuclear magnetic resonance measurement characterizing the rotation times for o-terphenyl. (For data sources used to construct part b, See Reference 3.)

increase, and the molecules that comprise it move more and more slowly. At some temperature the molecules move so slowly that they do not have a chance to rearrange significantly before the temperature is further lowered. Because these rearrangements are necessary for the liquid to find the equilibrium volume for that temperature, the experimentally observed V_{sp} will begin to deviate from the equilibrium value at this point. At a temperature not much lower than this, the structure of this material is “frozen” for practical purposes, and we call it a glass.

The change in the thermal expansion coefficient on cooling is one convenient way to define the glass transition temperature T_g . T_g depends on cooling rate, as a smaller cooling rate allows the sample to stay in equilibrium until lower temperatures. Notwithstanding its dependence on cooling rate, T_g is an important material property; for example, when defined consistently, it is the single parameter that is most useful in estimating the mechanical properties of a polymeric material. As observed in the laboratory, the glass transition is not a phase transition but rather a kinetic event that depends on the crossing of an experimental timescale and the timescale for molecular rearrangements. Glasses are not crystals or liquid crystals but are rather nonequilibrium solids without long-range order.

Supercooled liquids may be stable for very long times. For example, a pure sample of liquid *ortho*-terphenyl may not crystallize for years in a test tube at room temperature even though this is 35 K below its melting point. For atactic polymers (i.e. polymers with random stereochemistry), the crystalline state is often never obtained and may be higher in free energy than the liquid state at all temperatures. Supercooled liquids may be regarded as equilibrium states thermodynamically as long as no crystal nuclei are present.

Figure 1b shows some dynamic characteristics of supercooled liquids. The format for this plot was suggested by Angell (11) and provides a convenient way to compare the manner in which different liquids slow down as T_g is approached. The viscosity of three liquids is shown; viscosity is a macroscopic measure of the dynamics of a liquid. The viscosity increases dramatically as T_g is approached. For *o*-terphenyl, the viscosity increases 11 orders of magnitude in a 50-K range from room temperature down to T_g . Liquids like *o*-terphenyl, which show a strongly non-Arrhenius temperature dependence as T_g is approached, have been characterized by Angell as “fragile” liquids (11). Materials like SiO_2 , with a nearly Arrhenius temperature dependence, are known as “strong.” The timescale for molecular motion also increases dramatically as a supercooled liquid is cooled toward T_g . Nuclear magnetic resonance (NMR) measurements have characterized the rotation times for *o*-terphenyl (Figure 1b) (12). The rotation time at T_g is about 10^4 s; values between 10 and 10^4 s are typical for many low-molecular-weight molecular liquids. This is an astoundingly long time compared to the picosecond or nonosecond rotation times observed in “typical” liquids and in *o*-terphenyl itself above T_m . The molecular rotation time and the relaxation times associated with viscous flow and the enthalpy are typically similar in molecular liquids; these processes are collectively referred to as the α relaxation process. The close relationship between microscopic and macroscopic

measures of dynamics in supercooled liquids suggests that the study of microscopic dynamics will allow an understanding of the macroscopic properties of glass formers.

What Causes Slow Dynamics?

An important (and long-standing!) issue in this field is the origin of the slow dynamics observed as T_g is approached. Although not the primary focus of this review, some general comments may be useful. There is nothing surprising about dynamics slowing as the temperature is lowered; this happens catastrophically with the first-order phase transition from a liquid to a crystal. A fascinating aspect of dynamics in supercooled liquids is that the slow down occurs without an obvious structural cause. X-ray and neutron scattering studies of supercooled liquids generally show only subtle changes in local packing associated with a viscosity change of 12 orders of magnitude (13, 14); for hydrogen bonding liquids, larger changes in packing occur, but these are unlikely to be responsible for the slowing of dynamics as T_g is approached (15).

One class of explanations for viscous slowdown has focused on the volume change depicted in Figure 1a, arguing that an increase in density can account for sluggish molecular motion. Recent experiments have shown that this explanation can be rejected for some typical fragile glass formers; in the deeply supercooled region, the viscosity at constant density for these liquids is quite similar to the constant pressure behavior (16). These results argue that theories based on density changes, such as the free volume theory, are not fundamentally sound explanations of the low-temperature dynamics in fragile glass formers. Whether or not this conclusion rigorously extends to theories built upon density fluctuations [such as the idealized mode-coupling theory (17, 18)] is an interesting question (16).

If density changes are not responsible for sluggish dynamics near T_g , then temperature changes must somehow be responsible. A picture of simple activated dynamics is reasonable for SiO_2 . In this case, the temperature-independent activation energy is associated with the energy required to break Si–O bonds (bonds must be broken for flow to occur in this three-dimensional network). Here, lowering the temperature simply decreases the amount of energy available to cross a local barrier of fixed height. For fragile liquids like o-terphenyl, this simple picture fails because of the non-Arrhenius temperature dependence of dynamics. Fragile liquids may have apparent activation energies of 500 kJ/mol or more near T_g . As this surpasses the strength of chemical bonds in organic liquids, this activation energy is unlikely to be associated with motion of one molecule in a field of fixed neighbors. Often it is assumed that a group of molecules is rearranging in a cooperative manner. If this picture is correct, one would like to understand the nature of this motion and know how many molecules are involved in cooperative motion at various temperatures.

The Adam-Gibbs theory is one explanation built on cooperative dynamics. This theory derives a relationship between entropy and relaxation times that describes

a large number of experimental systems (19). Although this agreement with experiment is impressive (20, 20a) the validity of the Adam-Gibbs derivation is still a lively topic of discussion and thus the microscopic picture associated with this approach is not well established (20, 21). Recently Kivelson et al (22) proposed an alternate approach based on an avoided critical point associated with the formation of frustration-limited domains. As the temperature is lowered, this model assumes that molecules find a preferred local packing that cannot be extended indefinitely because it would not fill space efficiently. Local domains grow with decreasing temperature, and the large apparent activation energy is associated with these groups of molecules.

Connections with Technology

Much of the phenomenology of supercooled liquids and glasses transcends a particular class of materials. Molecules such as *o*-terphenyl (OTP) and glycerol are arguably the simplest systems that supercool and form glasses. These may be the ideal systems for uncovering the essential features of glass formation, and it is expected that insights from the study of these materials can be transferred to technologically more relevant systems, such as polymers, metallic glasses, aqueous solutions, and inorganic materials. As an example, most amorphous synthetic polymers are fragile glass formers and are similar to *o*-terphenyl in a plot like Figure 1a. Studies on low-molecular-weight glass formers potentially can explain the anomalously fast diffusion of solvents, antioxidants, and plasticizers through polymers (23), as well as some puzzling rheological properties (24, 25). Some current and future technologies involving information storage and photochromic switches depend on the isomerization kinetics of pendant groups or small molecules in polymers; these applications are certainly influenced by heterogeneities in dynamics that are qualitatively similar to those in low-molecular-weight glass-forming materials (26). Other areas where an understanding of mobility of supercooled liquids is essential include pharmaceuticals (will an amorphous drug crystallize during storage?) (27), enzyme and tissue preservation (can water be removed from a saccharide solution to yield a glassy matrix while preserving biological structures?) (28, 29), and food products (can crystallization of LifeSavers be suppressed?) (30).

SPATIALLY HETEROGENEOUS DYNAMICS

Looking back over the past several decades, the most compelling reason to examine the possibility of spatially heterogeneous dynamics comes from the observation of nonexponential relaxation processes. For fragile glass formers like OTP, it is generally observed that correlation and relaxation functions associated with molecular motion (such as those observed in dielectric relaxation or NMR spectroscopy) become increasingly nonexponential as T_g is approached from above. Often these

relaxation functions are fit to the Kohlrausch-Williams-Watts (KWW) or stretched exponential equation:

$$CF(t) \approx \exp[-(t/\tau)^\beta]. \quad 1.$$

For a typical fragile glass former, β decreases from near 1 at high temperature to about 0.5 near T_g . Nonexponential relaxation has two fundamentally different explanations. One can imagine that a heterogeneous set of environments exists in a supercooled liquid; relaxation in a given environment might be nearly exponential, with the relaxation time varying significantly among environments. Alternatively, one can imagine that supercooled liquids are homogeneous and that each molecule relaxes nearly identically in an intrinsically nonexponential manner. In this scenario, one might associate a decreasing β with increasing cooperativity. The two possible explanations can be expressed in another way. The inverse Laplace transform of the correlation function is the probable density function $G(\tau)$ such that

$$CF(t) = \int_0^\infty G(\tau)e^{-t/\tau} d\tau. \quad 2.$$

The heterogeneous explanation says that $G(\tau)$ represents a spatial distribution of relaxation times whereas the homogeneous explanation argues that $G(\tau)$ has no direct physical interpretation.

The basic idea in the preceding paragraph could have been stated any time in the past 60 years. Only in the past 10 years, however, have experiments been developed that allow the two explanations to be clearly tested. In my opinion, these experiments make a compelling case that the heterogeneous picture is correct and I write this review from this viewpoint. For some experiments, homogeneous explanations have also been advanced and these are noted below.

A number of groups have performed large molecular dynamics computer simulations of supercooled liquids and characterized spatially heterogeneous dynamics in these model systems (31–34). Such simulations provide possible scenarios for dynamics in deeply supercooled liquids. Figure 2a shows the simulation results of Hurley & Harrowell (35) for a two-dimensional system of soft disks. The positions of particles are plotted at many times. Clearly there are regions of the sample where the local structure has remained constant, while over the same time period, other parts of the sample have rearranged significantly. Other simulations find qualitatively similar results. Donati et al (36) have reported large loops of mobile particles in three-dimensional simulations of Lennard-Jones spheres; particles in these loops move substantially whereas all around this loop the structure is fixed. Although these simulations have provided considerable insight into spatial heterogeneities in dynamics, two important limitations need to be stated. First, most of these simulations have been limited to “molecules” that are much simpler in structure than are the molecular liquids studied in the laboratory. Second, the simulations are limited to relaxation times of roughly 100 ns, whereas relaxation times in typical laboratory experiments exploring spatially heterogeneous dynamics are

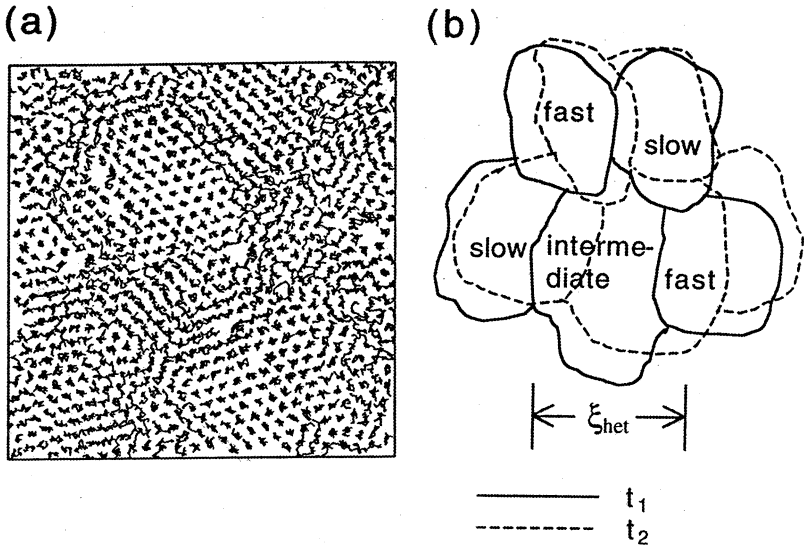


Figure 2 Images of spatially heterogeneous dynamics. (a) Overlaid maps of particle positions at various times from a two-dimensional simulation of soft disks (35). Regions in which distinct particles are easily visible have a fixed structure over this time period. Other regions show substantial rearrangement of local structure on the same timescale. Dynamics in such simulations are much faster than are dynamics near the laboratory T_g , so heterogeneous dynamics near T_g may be different from the image shown. (Reprinted from Reference 35 by permission.) (b) Schematic illustration of regions of spatially heterogeneous dynamics near T_g . These regions are on the order of ξ_{het} in dimension (typically a few nanometers) and evolve in time.

on the order of 1 s. Thus the simulations explore heterogeneities far above T_g in a regime where experiments find little evidence for heterogeneous dynamics. For these reasons, the results of simulations like those shown in Figure 2a should be considered as suggestive but not conclusive when considering spatial heterogeneity near T_g .

Figure 2b shows a cartoon of spatially heterogeneous dynamics near T_g . Although regions of different dynamics are distinguished by sharp lines in this sketch, current experiments do not distinguish between this and a continuous evolution of relaxation rates from one region to another. Figure 2b immediately brings to mind a number of questions. How large are these heterogeneities? How much do the dynamics vary between the fastest and slowest regions? How long do they last? And where do they come from? The focus of this review is a description of the experiments that led to Figure 2b, and a status report on the answers to each of these questions. As a brief preview, the experiments indicate a characteristic size of these regions of roughly 3 nm and dynamics that differ by 1–5 orders of magnitude between the fastest and slowest regions at T_g . Molecules

that are in slow domains at some particular time are likely to remain slow at least as long as the average relaxation time of the system, and possibly much longer. The origin of the spatial heterogeneity in dynamics is not clearly established.

Dynamic Hole-Burning Experiments

How does one determine whether dynamics in a supercooled liquid are heterogeneous or homogeneous? As described above, observation of ensemble average relaxation functions (i.e. two-time correlation functions) do not usually allow this determination to be made because either scenario is consistent with a nonexponential relaxation function. Hole-burning experiments provide one approach to this question. In a standard hole-burning experiment, a broad absorption line is selectively excited by a narrow excitation line. The subsequent observation of a “hole” in the absorption spectrum at the frequency of excitation is sufficient to establish that the absorption line is inhomogeneously broadened, i.e. a heterogeneous distribution of environments exists in the sample. In the past decade, three dynamic hole-burning experiments have been developed and used to investigate supercooled liquids (37–39). Each of these techniques allows the dynamics of subensembles to be selectively observed, e.g. only the slow regions in Figure 2*b*. The observation of a subensemble with dynamics different than the overall ensemble is sufficient to establish that dynamics are heterogeneous. Note that a dynamic hole-burning experiment perturbs the distribution of relaxation times whereas a standard hole-burning experiment perturbs the distribution of absorption frequencies. The analogy is not perfect and some prefer the term dynamic filter to dynamic hole-burning.

The first experiment of this type was performed by Schmidt-Rohr & Spiess (37) using solid-state NMR. Their reduced four-dimensional NMR experiment measures some parts of a four-time correlation function and conceptually works as follows. The experiment first selects a group of C-H vectors that have changed orientation by an unusually small angle during the time interval between t_1 and t_2 . After some waiting time, this same subset is interrogated (between time t_3 and t_4 , with $t_4 - t_3 = t_2 - t_1$) to determine whether these vectors have again changed orientation by an unusually small angle. Schmidt-Rohr & Spiess showed for poly(vinylacetate) at $T_g + 10$ K that the initially selected slow subset remained slow if the waiting time was short, indicating that dynamics are indeed heterogeneous. After a very long waiting time, the slow subset had evolved into an average set of C-H vectors. This is a requirement for an ergodic system in which time and ensemble averages are equivalent. The characteristic time for a slow subset to remain slow was determined to be comparable to the average relaxation time of the slow subset. Thus, not only did this experiment establish that dynamics are heterogeneous, for one system at one temperature it also measured the lifetime of the heterogeneities. Later work extended this experiment to o-terphenyl (40), glycerol (41), and toluene (42). Altogether, these experiments on polymeric

(43, 44) and low-molecular glass-forming liquids at temperatures from $T_g + 10$ K to $T_g + 20$ K yielded similar results; slow subsets could be selected and their lifetimes were comparable to their average relaxation time.

In 1995, Cicerone & Ediger (38) reported an optical version of a dynamic hole-burning experiment. In these optical experiments, the reorientation of a dilute probe molecule (<100 ppm) is monitored. In this case, the probe was tetracene, which is similar in size and chemical functionality to OTP the host (structures shown in Figure 3). Probe reorientation on the second and kilosecond timescale can be observed via photobleaching (45), as illustrated in Figure 3. This technique relies on the observation that in the presence of oxygen, tetracene and similar probes undergo permanent photobleaching (photo-peroxidation) with a quantum efficiency of about 10^{-4} . If the sample is illuminated for a few milliseconds with

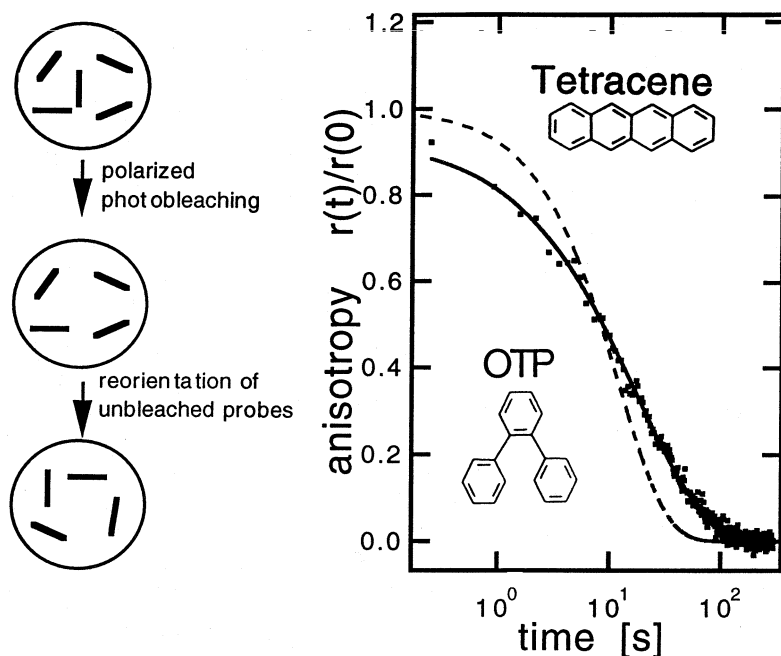


Figure 3 Photobleaching experiment to measure slow reorientation. (*Left*) Polarized photobleaching selectively destroys molecules whose transition dipoles are parallel to the laser polarization. Subsequent reorientation of the chromophores can be monitored by polarized optical absorption with fluorescence detection. (*Right*) Reorientation data for tetracene in o-terphenyl (OTP) at a few degrees above T_g . At short times, the anisotropy is high because of polarized photobleaching. After about 100 s, the tetracene molecules have completed randomized their orientation and the anisotropy function decays to zero. This decay can be well fit to a stretched exponential function (Equation 1) with $\beta = 0.6$ (Dashed line) A fit to an exponential function ($\beta = 1$).

light from an Ar⁺ laser, a small fraction of the probes will be photobleached. If this laser light is polarized and molecular motion is slow, the transition dipoles of the unbleached probes will be preferentially oriented perpendicular to the laser polarization. This anisotropic subset will become a random subset on the timescale of probe reorientation. Subsequent illumination of the sample with a weak reading beam whose polarization is modulated allows the decay of the probe anisotropy to be monitored in time, as shown in Figure 3. The anisotropy decay is well fit by the KWW equation (Equation 1), and an average rotation time τ_c can be calculated from the integral of the correlation function. Although this technique directly observes the reorientation of probe molecules, it has been shown that the reorientation of tetracene in OTP is very similar to NMR measurements of the reorientation of OTP itself (46).

The optical dynamic hole-burning experiment (Figure 4*a,b*) is slightly more complicated than the photobleaching experiment described above. First the sample was illuminated with unpolarized light for a length of time sufficient to destroy 60% of the tetracene molecules. At various periods after this deep photobleach, the shallow bleaching experiment described above is performed. For short waiting times Δt , the subset remaining after the deep bleach was observed to have an average rotation time longer than the original ensemble. For long enough waiting times, the remaining subset showed the same average rotation time as the original ensemble. The results of Cicerone & Ediger together with more recent work by Wang & Ediger (47), are shown in Figure 4*c*. At $T_g + 1$ K, and immediately following the deep bleach, the surviving group of probes rotated 35% slower than the original ensemble of probes. Eventually, at times approaching $10^4 \tau_c$, the surviving probes have become an average subset in terms of their rotational correlation time. The decay of this curve defines τ_{ex} , the characteristic exchange time, so named because molecules must exchange their dynamic environments in order for this function to decay. At $T_g + 4$ K, the randomization of dynamic environments is much faster, on the order of $10 \tau_c$.

The alert reader will note that the exchange times from the optical experiment are much longer than the results from the reduced four-dimensional NMR experiment (40). This is a matter of considerable controversy. One resolution is shown in Figure 5*a*, where the ratio of the exchange time to the α relaxation time is shown for OTP as a function of temperature (note $\tau_\alpha \approx \tau_c$ for tetracene). As shown, the optical and NMR results [from Bohmer et al (40)] can be reconciled if τ_{ex}/τ_α shows a very strong temperature dependence that begins only a few degrees above T_g . Another resolution is to discount the optical deep bleaching results because only probe dynamics are observed. The close correspondence between the rotation of tetracene and that of OTP itself over a large temperature range is an argument against this point of view (45). Wang & Ediger (48) recently reported deep bleaching experiments for two probes in polystyrene. The exchange times from these measurements (Figure 5*b*) also show a strong temperature dependence to τ_{ex}/τ_α , indicating that the existence of long exchange times is neither probe nor matrix specific.

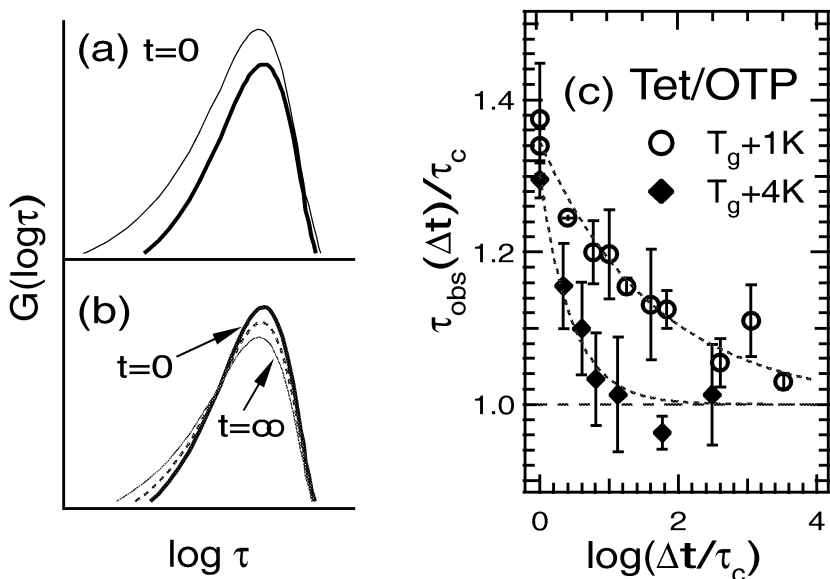


Figure 4 Photobleaching measurement of lifetime of slow domains. (a) When a significant fraction of probe molecules are photobleached, probes in more mobile environments are bleached with a higher efficiency. Thus the remaining probes have a distribution of rotation times that is skewed toward long times (*bold line*) relative to the initial distribution (*narrow line*). (b) With time, the slower-than-average subset of probe molecules evolves into a subset with the same distribution of rotation times that characterized the initial ensemble. (c) As the slower-than-average subset shifts toward equilibrium, the average rotation time of the subset shortens and finally reaches the value that characterized the initial ensemble. Here results are shown for tetracene in o-terphenyl (OTP) at two different temperatures. In both cases, the subset of probes that remained after deep photobleaching rotated about 30% slower than did the overall ensemble. The decay of this curve defines τ_{ex} , the characteristic time for exchange of dynamic environments. (Data from Reference 47.)

In 1997, a dielectric version of the dynamic hole-burning experiment was reported by Schiener et al (39). The linear dielectric response of a material may be observed if the polarization is monitored following the application of a small voltage across a capacitor containing a liquid. In the dielectric hole-burning experiments, a large oscillating electric field at a frequency ω is first applied to the sample, and then after some waiting time, the linear experiment is performed. By performing the experiment with a series of phase changes, the frequency-dependent dielectric spectrum of the perturbed liquid is obtained as a function of waiting time and the excitation frequency ω . Schiener et al (39) reported results for two supercooled liquids, propylene carbonate and glycerol. In each case, holes

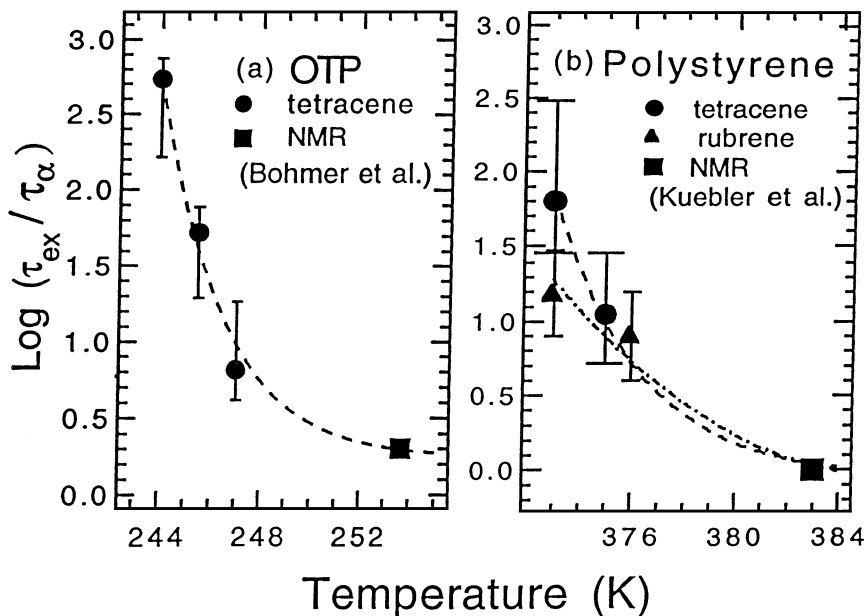


Figure 5 Exchange times, ratioed to the alpha relaxation time, as a function of temperature in o-terphenyl (OTP) and polystyrene. In both systems, $\tau_{\text{ex}}/\tau_{\alpha}$ is a strong function of temperature near T_g , and roughly equal to unity above $T_g + 10$ K. Thus near T_g , molecules have a long memory of their dynamic environment relative to the average rotation time. (Data from References 47 and 48.)

in the dielectric spectrum were observed at the frequency ω for sufficiently short waiting times. In agreement with the optical and NMR experiments, this argues that dynamics in the sample are heterogeneous. For both samples at T_g , the holes were observed to fill without noticeable broadening on the time scale of the τ_{α} . Two interpretations have been given to this result. One opinion states that the hole filling is associated with exchange, and therefore τ_{ex} is comparable to τ_{α} , even at T_g . The other view holds that hole broadening is the signature of dynamic exchange, just as spectral diffusion in an ordinary hole-burning experiment is taken as evidence of site exchange. This second view concludes that $\tau_{\text{ex}}/\tau_{\alpha}$ is larger than unity and possibly much larger.

Very recently, Cugliandolo & Iguain have shown that some observations of the dielectric hole-burning experiment can be reproduced by a model that has no spatial structure and thus no spatial heterogeneity (48a). Such alternate explanations help to refine our understanding of the information content of these experiments. Nevertheless, it seems unlikely that similar homogeneous explanations of the NMR and optical experiments will emerge as viable alternatives to the heterogeneous view.

Other Experiments that Measure Lifetimes of Heterogeneous Domains

Dynamic hole burning is not the only approach to selecting a subensemble with dynamics different than the entire ensemble. If experiments can be performed on a sufficiently small volume of a spatially heterogeneous system, the dynamics in the small volume will be observed to fluctuate as a function of time if the system is ergodic. Such an experiment has been reported by Russell et al (4). An atomic force microscope tip was held fewer than 10 nm above a sample of polyvinylacetate near T_g . The resonance frequency of the cantilever holding the tip was observed to fluctuate with time. These fluctuations were interpreted as resulting from fluctuations of the dielectric properties of a region of the sample within about 50 nm of the surface. The observed fluctuations are consistent with spatially heterogeneous dynamics that persist about twice as long as τ_α near T_g . It is not clear whether the data excludes longer-lived heterogeneity at lower temperatures. This experiment also estimated the size of dynamic domains at roughly 10 nm. As discussed below, this is somewhat larger than estimates from other measurements.

A logical extension of the above strategy is to measure the dynamics of individual molecules. Although this is probably not possible for a single molecule in a one-component system, it would be possible for isolated chromophores in a glass-forming matrix. Single-molecule studies of molecular orientation have been performed (50, 51), and it seems likely that a characteristic time for changes in orientation can be determined for individual dye molecules. If such a characteristic time for reorientation could be determined several times for a given dye before photobleaching occurs, many aspects of heterogeneous dynamics could be investigated. Alternately, changes in some other property connected with probe mobility could be monitored. Recent work by Ishikawa et al (52) suggests that temporal fluctuations in the fluorescence lifetime of "rotor probes" might be observable.

Solvation dynamics experiments can also be sensitive to spatial heterogeneities in dynamics. Richert and coworkers (53–57) have shown that the time-resolved phosphorescence spectrum of a dipolar chromophore can be used to monitor the local dielectric response of the solvent. For quinoxaline in 2-methyltetrahydrofuran (53, 54), and several other glass-forming systems (55), the ensemble-averaged local solvation response is equivalent to results obtained from macroscopic dielectric relaxation measurements. Because the entire phosphorescence spectrum can be acquired as a function of time, this experiment is sensitive not only to the ensemble-average relaxation but also to the distribution of relaxation rates around different chromophores; changes in the width of the spectrum with time indicate heterogeneity in the local relaxation rates (56, 57). Figure 6 shows results using this technique for quinoxaline in 2-methyltetrahydrofuran over the temperature range from T_g to $T_g + 6$ K. The ordinate reports changes in the width of the spectra normalized to ensemble average relaxation behavior. The fact that this quantity continues to increase at long times, rather than become constant, as predicted by

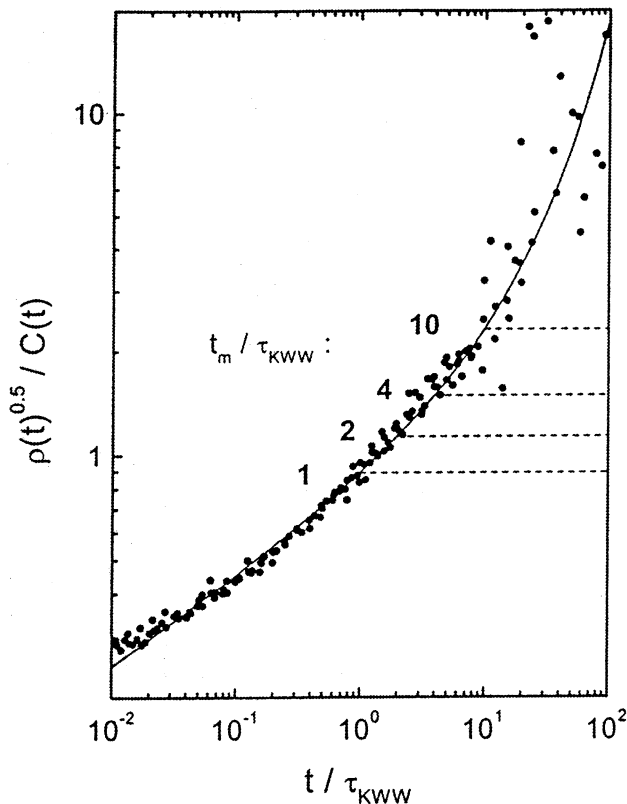


Figure 6 Master plot of data from solvation dynamics experiments (57) on quinoxaline in 2-methyltetrahydrofuran, with data from T_g to $T_g + 6$ K. $C(t)$ is the Stokes shift correlation function and $\rho(t)$ represents the variance of the local contributions to this function. The data at all experimentally accessible times are consistent with completely heterogeneous relaxation (solid line), i.e. no exchange of dynamic environments. Exchange of dynamic environments on various time scales t_m/τ_{KWW} would lead to the horizontal dashed lines. Because the data do not follow these dashed lines, exchange of dynamic environments must happen on longer timescales. (Reprinted with permission from Reference 57.)

a model with exchange of dynamical environments, indicates that $\tau_{ex}/\tau_\alpha \geq 25$ for this system (57). Although these measurements do not show the strong temperature dependence of Figure 5, they do indicate an extremely long exchange time, consistent with the data at lower temperatures in Figure 5.

The issue of the lifetime of the regions is an important one because it has a strong impact on how we think about heterogeneous dynamics. If τ_{ex} is always compared with τ_α , then the heterogeneity in dynamics should be thought of as just another aspect of the α relaxation process (58). If, in contrast, $\tau_{ex} \gg \tau_\alpha$, then a new relaxation process (τ_{ex}) needs to explicitly enter our phenomenological description

of dynamics near T_g . The strong divergence of τ_{ex} near T_g could suggest that spatially heterogeneous dynamics are at the center of the problem of understanding the cause of slow dynamics as T_g is approached.

Overall, the experimental situation regarding the lifetimes of regions of heterogeneous dynamics is not clear. If the results indicating that $\tau_{\text{ex}}/\tau_{\alpha} \gg 1$ are accepted as correct, one must ask why this behavior is universal in any sense or even common? The significance of these observations awaits additional measurements. Unfortunately, most existing methods for determining the heterogeneity lifetime work in only a small temperature range or have other restrictions that make them not generally applicable. The development of new experimental approaches could provide significant clarification.

How Big Are the Heterogeneities?

The experiments described above argue strongly that dynamics are heterogeneous and that these heterogeneities persist at least as long as the ensemble average relaxation time. However, these experiments do not give much indication of the spatial scale of the heterogeneities. If a “slow” molecule is picked at random, one expects that its neighbors are also reasonably slow, but at sufficiently long distances molecules with all types of dynamics must be found. What is the characteristic length scale for this correlation, denoted ξ_{het} in Figure 2*b*?

Although many indirect or model-dependent methods have been used to estimate ξ_{het} (59–65), there is one experiment that directly measures ξ_{het} . Tracht et al (66) have developed a variation of the reduced four-dimensional NMR experiment (described above) that accomplishes this. This experiment depends on transfer of magnetization between ^{13}C and ^1H nuclei via cross polarization, a process that is only efficient if the two nuclei are within 3 Å of each other. The experiment again begins by applying a filter that leaves ^{13}C magnetization only on nuclei in regions where C-H vectors have reoriented by unusually small angles. This magnetization is transferred to protons and allowed to diffuse from immobile regions toward mobile regions. After various diffusion times, magnetization is transferred back to ^{13}C nuclei, and the fraction of these nuclei in immobile regions is determined. With increasing diffusion time, smaller fractions are observed until the decay hits a plateau, when the magnetization is found in a random set of dynamic environments. The characteristic time for loss of memory about the initial slow subset can be converted to the characteristic length for heterogeneous dynamics using the spin diffusion coefficient (66). Figure 7 shows data reported by Tracht et al (66) for polyvinylacetate at $T_g + 10$ K. The data are consistent with ξ_{het} in the range from 2–3 nm.

Clearly one would like to understand how this length scale changes with temperature and how it depends on the chemical identity of the glass formers. Several theories of the glass transition invoke an increase in a structural or dynamical correlation length as T_g is approached from above. In the Adam-Gibbs treatment, for example, a length scale for cooperative dynamics (ξ_{coop}) is predicted to grow with

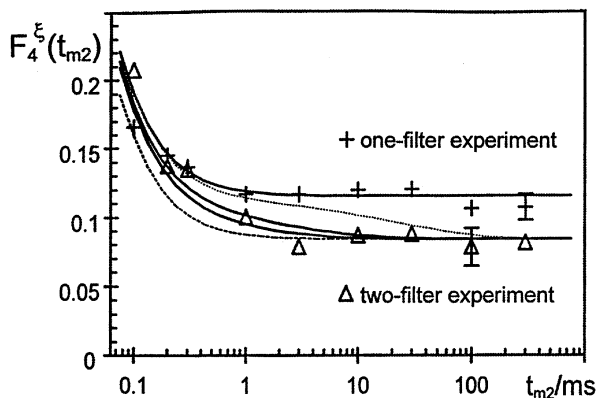


Figure 7 Solid-state NMR measurements (66) of the size of regions of heterogeneous dynamics ξ_{het} for polyvinylacetate at $T_g + 10$ K. Data are shown for experiments using spin diffusion (one-filter experiment, used to obtain spin diffusion coefficient) and using both spin diffusion and dynamic selection (two-filter experiment). The two-filter experiment decays somewhat slower than the one-filter experiment, indicating that ξ_{het} is larger than the average distance between ^{13}C labels in the system. Fitting indicates that ξ_{het} is in the range of 2–4 nm. (Reprinted with permission from Reference 66.)

decreasing temperature; this length defines the smallest region that can rearrange independent of its neighbors (19). Although heterogeneous dynamics are not discussed by Adam and Gibbs, it would be reasonable to equate ξ_{het} with ξ_{coop} . Even if these two lengths are not synonymous, ξ_{het} should place an upper bound on ξ_{coop} because it makes no sense to say that dynamics are orders of magnitude different 3 nm from a given molecule if the cooperativity length is 5 nm. Thus, measurements of ξ_{het} as a function of temperature for various materials may provide crucial information about the fundamental origin of slow dynamics near T_g .

TRANSLATIONAL DIFFUSION IN SYSTEMS WITH SPATIALLY HETEROGENEOUS DYNAMICS

In 1992, Fujara et al (67) reported the remarkable result that translational diffusion in OTP has a weaker temperature dependence than the viscosity of the liquid or its rotational correlation time. This data is shown in Figure 8. The rotational correlation times were obtained via NMR measurements on deuterated OTP. At high temperatures, self-diffusion coefficients were determined with field-gradient NMR methods, whereas at low temperatures, where NMR measurements are not possible, the translational diffusion coefficients of two dilute probes are plotted. Subsequently, Cicerone & Ediger (46) reported rotation and translation measurements of tetracene in OTP, shown in Figure 9. Because the rotation and translation

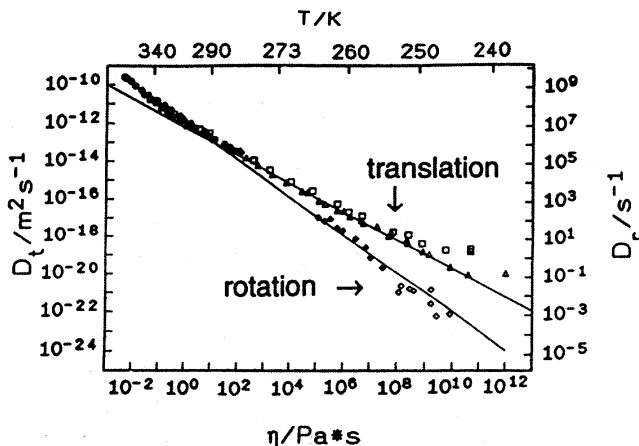


Figure 8 Translational (D_t) and rotational ($D_r = 6/\tau_c$) diffusion coefficients in o-terphenyl (12) as a function of viscosity and temperature. Translation: self-diffusion (*solid circles*); tracer diffusion for two probes (*open box* and *open triangle*). Rotation: self-diffusion for deuterated o-terphenyl (*filled* and *open diamonds*). Full lines show $\eta^{-0.75}$ and η^{-1} dependences. Translational diffusion has a weaker dependence on viscosity below 290 K than above. Translational and rotational diffusion have different temperature dependences below 290 K. (Adapted from Reference 12 and used with permission.)

of the same molecule are compared here, this data emphasizes that the dramatically different temperature dependences for rotation and translation in Figure 8 cannot be ascribed to the fact that rotation of one molecule (OTP) was being compared with translation of another (a probe). [Over the range where rotation and translation measurements can be made on neat OTP, these results are in good accord with the probe results shown in Figure 9 (46).]

If one imagines that dynamics in OTP are homogeneous, then the data shown in Figures 8 and 9 lead to two conclusions [which I believe are incorrect (see below)]. First, the relaxation of structure (the viscosity) is apparently not determined by diffusion of molecules! Second, because both rotation and translation experiments measure single-particle correlation times, this data apparently indicates that the distance translated per rotational correlation time increases significantly from high temperature to T_g ; although at high temperatures molecules translate about half a diameter in the time required to rotate 45° , near T_g translation of 10 diameters would be required in the time needed to rotate 45° . I emphasize that these conclusions follow from the data only if dynamics are assumed to be homogeneous.

Tarjus & Kivelson (68) first articulated the alternate explanation of Figures 8 and 9 provided by the assumption of spatially heterogeneous dynamics, although elements of this approach had been suggested earlier (12, 69, 69a). In such a heterogeneous system, care must be taken to consider the way in which

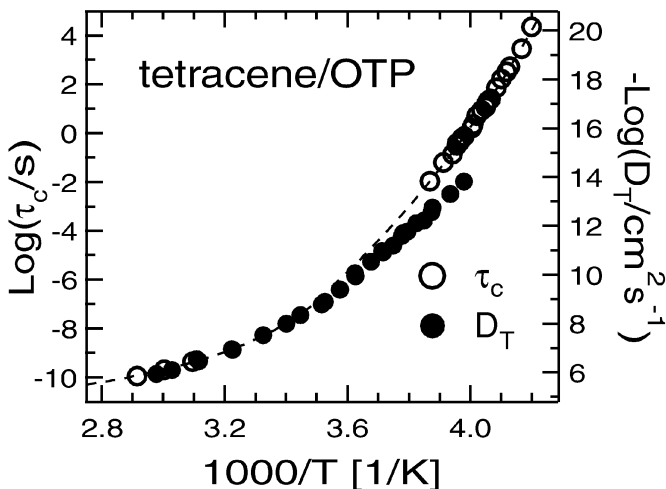


Figure 9 Translational diffusion coefficients (D_T) and rotational correlation times (τ_c) for tetracene in *o*-terphenyl (OTP). At high temperature, these two quantities have the same temperature dependence, whereas at low temperature, D_T has a weaker temperature dependence than does τ_c . (Data from Reference 46.)

the rotation and translation experiments average over the heterogeneity. Let the spatial distribution of local rotation times be given by $\rho(\tau)$; further, assume that local translational mobility is proportional to local rotational mobility, i.e. regions of fast rotation are also regions of fast translation (70). As discussed below, the rotation and translation experiments are sensitive to different moments of this distribution. To a first approximation the rotation experiment measures $\langle \tau \rangle$ while the characteristic time to translate a given distance is roughly proportional to $\langle \tau^{-1} \rangle^{-1}$. If the width of $\rho(\tau)$ increases with decreasing temperature, then the translational diffusion coefficient will have a weaker temperature dependence than the rotational correlation time.

Why do the rotation and translation experiments average over heterogeneity in different ways? The orientation correlation function in such a system is an average of the correlation functions for the different regions of the sample. Molecules in more mobile regions reorient quickly and are responsible for the fast initial decay in the correlation function whereas molecules in less-mobile regions are responsible for the long tail of this function. Because the rotational correlation time is the integral of the correlation function, and the integral is more sensitive to the long tail than to the initial fast decay, τ_c selectively provides information about regions of slower-than-average mobility. In contrast, the long time translational diffusion coefficient emphasizes regions of high mobility. This result is not so obvious, and it is useful to first consider a counter-example. In a system with alternating layers of fast and slow diffusion (Figure 10a), the long time diffusion coefficient D_T

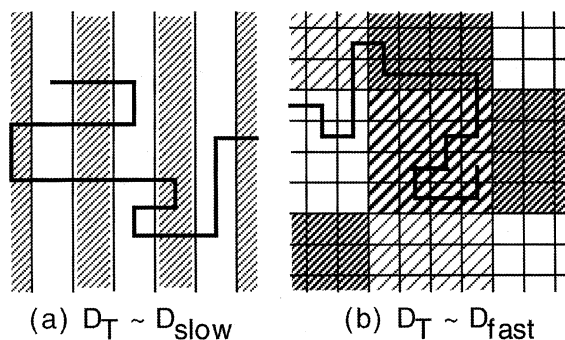


Figure 10 Schematic representation of translational diffusion in heterogeneous media. (a) Transport horizontally is limited by the slow regions because these regions must be traversed to move a large distance horizontally. (b) Transport is determined by the fastest diffusion coefficients because many paths allow molecules to move around slow regions.

perpendicular to the layers is determined by the diffusivity of the slow regions. This is intuitively obvious, as the slow regions must be traversed in order for the molecules to travel a large distance in this direction. Now consider a three-dimensional system where regions of different mobility form a random patchwork as shown in Figure 10*b*. In this case, molecules have the option of flowing around regions of slow mobility, and these paths dominate the determination of the long time diffusion behavior. Qualitatively, this is similar to a three-dimensional network of randomly chosen resistors; most of the current follows paths of lower-than-average resistance. These qualitative arguments are supported by analytical calculations for a two-state system in the effective medium approximation (71, 72) and numerical simulations of a quasi-continuous distribution of local relaxation times (73). Elements of this explanation have been confirmed in molecular dynamics simulations of two-dimensional liquids (74).

The heterogeneous explanation of Figures 8 and 9 avoids the physically unappealing conclusion that translational diffusion is decoupled from molecular rotation and structural relaxation. But is it correct? There are two strong arguments in favor of the heterogeneous interpretation of these figures. The first is shown in Figure 11, where data for the translational and rotational mobility for probes in five different glass formers at T_g are collected (75). The abscissa plots the KWW β parameter for probe rotation while the ordinate indicates the number of orders of magnitude by which translational diffusion at T_g exceeds the value expected in a homogeneous system. The heterogeneous explanation makes the qualitative prediction that a correlation should exist between these quantities because both axes are a measure of spatially heterogeneous dynamics in the system. The experimental data clearly supports this view. Torkelson and coworkers have shown that the same correlation exists when considering one polymer/probe system as a function of temperature (76), which further supports the view that spatially heterogeneous dynamics are

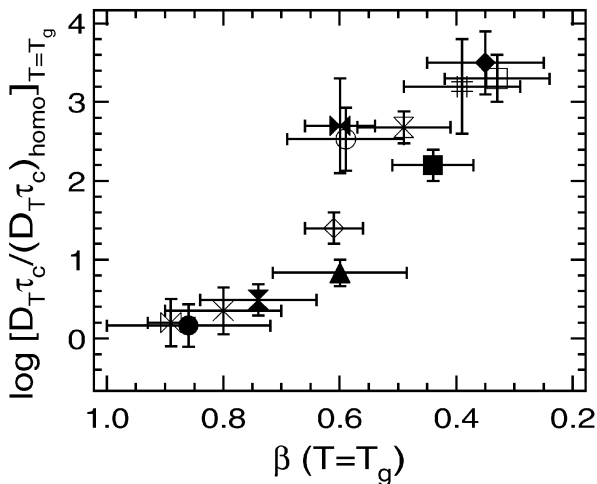


Figure 11 Comparison of enhanced translation ($D_T \tau_c$) with the KWW β parameter at T_g for probes in five glass-formers: o-terphenyl, tris(naphthyl)benzene, polystyrene, polysulfone, and polyisobutylene. The *vertical axis* scales the experimental results to the result expected for motion in a homogeneous continuum. The correlation shown is expected if both enhanced translation and nonexponential rotation are due to spatially heterogeneous dynamics. (Data sources given in Reference 75.)

responsible for both enhanced translation and nonexponential reorientation. It is interesting that the system in Figure 11 that appears most homogeneous on this plot (near the *lower left corner*) is also the least fragile of the glass formers in this group.

The second argument in favor of the heterogeneous explanation of Figures 8 and 9 comes from recent translational mobility measurements of tetracene in polystyrene by Wang & Ediger (77). The technique of holographic fluorescence recovery after photobleaching used in these experiments measures the intermediate scattering function for probe translation:

$$\frac{S(q, t)}{S(q, 0)} = \int_{-\infty}^{\infty} G_s(x, t) e^{iqx} dx. \quad 3.$$

Here $G_s(x, t)$ is the self part of the van Hove function, giving the probability that a particle has moved a distance x in a time t . For Fickian diffusion, the van Hove function is given by

$$G_s(x, t) = \frac{1}{\sqrt{4\pi D_T t}} \exp(-x^2/4D_T t), \quad 4.$$

where D_T is the long time diffusion coefficient. Substitution of Equation 4 into Equation 3 yields the intermediate scattering function assuming Fickian diffusion:

$$\frac{S(q, t)}{S(q, 0)} = \exp(-q^2 D_T t). \quad 5.$$

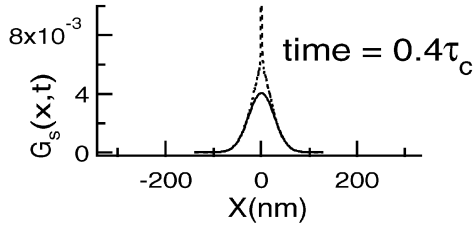


Figure 12 KWW β parameter for the intermediate scattering function $[S(q,t)]$ observed for tetracene translation in polystyrene ($q = 0.042 \text{ nm}^{-1}$). A β parameter of unity is consistent with Fickian diffusion. As the temperature is lowered, increasingly non-Fickian diffusion is observed. A lattice simulation based on Figure 10b can roughly reproduce the observed β parameters. (Inset) A van Hove function from this simulation together with a Gaussian fit; a Gaussian function is expected for Fickian diffusion. This van Hove function from the simulation indicates that many molecules have not left their initial site even though most molecules have moved more than 50 molecular diameters. (Data and simulation results from Reference 77.)

Wang & Ediger fit the intermediate scattering function as a function of temperature to the KWW function (Equation 1). As shown in Figure 12, the observed decays were consistent with Fickian diffusion ($\beta = 1$) at high temperature but were clearly nonexponential at lower temperatures. Because the wavevector used in this experiment corresponds to a length scale ($2\pi/q$) of 150 nm, these results indicate substantial deviations from Fickian diffusion on large length scales. Modeling of translational diffusion in a heterogeneous system (Figure 10b) was able to reproduce this data reasonably well (73); Figure 12 shows the van Hove function predicted by the model for $t = 0.4 \tau_c$. Note the substantial deviations from a Gaussian shape even when most molecules have moved more than 25 nm from their initial position. In contrast, computer simulations (78) and neutron spin echo experiments (79) of liquids far above T_g indicate Fickian diffusion when molecules have moved less than 1 nm. This substantial influence of spatially heterogeneous dynamics on translational motion near T_g is completely consistent with the heterogeneous interpretation of Figures 8 and 9.

Ngai recently used the coupling model to provide an alternate, homogeneous explanation for experimental observations of enhanced translational diffusion (79a). Experimental observations of non-Fickian translation (Figure 12) have not yet been addressed with this approach.

Implications of Heterogeneous Interpretation of Enhanced Translational Diffusion

One important implication of the heterogeneous explanation of Figures 8 and 9 is that the spatial distribution of local relaxation times at T_g must be orders of magnitude in width. Otherwise, the different moments of this distribution would not

differ enough to account for enhancements in translational diffusion of more than three orders of magnitude. The correlation shown in Figure 11 argues that spatially heterogeneous dynamics are the primary cause of nonexponential relaxation functions observed at T_g for fragile glass formers (73). For a KWW function with $\beta = 0.5$, the FWHM of the probability density is 1.6 decades; for $\beta = 0.35$, the FWHM is 2.7 decades. This conclusion is consistent with the conclusions of the reduced four-dimensional NMR experiments, the dielectric hole-burning experiments, and the solvation dynamics experiments (80). In particular, the solvation dynamics experiments (57) have been interpreted as indicating that the correlation function response within any given dynamic environment is nearly exponential (KWW $\beta = 1.00 \pm 0.08$). Thus, although we argued earlier that nonexponential ensemble average relaxation function need not necessarily indicate a system with strong heterogeneities, currently available evidence supports the view that at least near T_g , the $G(\tau)$ inferred from ensemble average measurements (Equation 2) does represent the spatial distribution of mobilities. As the KWW β parameter is known to correlate with fragility (81), this leads to the inference that strong glass formers are more homogeneous than fragile glass formers.

Another implication of the heterogeneous interpretation of the enhanced translation effect is that the width of the spatial distribution of relaxation times must have a strong temperature dependence (23, 76). For OTP, the data shown in Figures 8 and 9 indicates essentially homogeneous dynamics at temperature above about $1.2 T_g$. Other systems show similar behavior (12, 82–86). This observation is one reason that high-temperature simulation results such as those shown in Figure 2a do not necessarily provide insight into spatially heterogeneous dynamics near the laboratory glass transition.

One can interpret the temperature dependence of heterogeneous dynamics in terms of a picture developed by Goldstein, who argued more than 30 years ago that diffusion in liquids occurs by different mechanisms at high and low temperatures (87). In his view, molecules at low temperature move by crossing substantial potential energy barriers (i.e. activated transport or hopping). At high temperatures, thermal energies will be comparable to the barrier heights and translational motion will have a fundamentally different character (free diffusion). Goldstein argued that the transition from free to activated diffusion should occur when the relaxation time for the shear viscosity is about 10^{-9} s and the viscosity is about 10 P; this coincides roughly with the temperature at which the enhancement of translational diffusion begins, and also with the critical temperature T_c in the idealized mode-coupling theory. This suggests the following possible interpretation (88). High-temperature dynamics are nearly homogeneous, and explanations such as mode-coupling theory can be reasonably successful. Low-temperature dynamics are strongly heterogeneous, as the existence of barriers not only slows transport but also allows a distribution of barrier heights to be easily envisaged. Aspects of this interpretation have recently been confirmed for one model liquid by computer simulation (89, 89a). This explanation also suggests that the interpretation of the

KWW β parameter as indicating spatial heterogeneity may not be applicable at temperatures far above T_g .

It is interesting to note that the most dramatic evidence for anomalies in translational motion in supercooled liquids has come from studies involving probe molecules. With the exception of a recent study of supercooled water by Smith & Kay (90), essentially no self-diffusion measurements are available for molecular liquids near T_g . Field-gradient NMR methods have been used to measure self-diffusion coefficients down to 10^{-10} cm²/s in many liquids, but this is roughly six orders of magnitude larger than the value expected at T_g . The development of techniques that can measure self-diffusion down to T_g in a variety of molecular liquids would be very useful.

WHY ARE DYNAMICS SPATIALLY HETEROGENEOUS?

Of the various questions considered in this paper, the answers to this question are the most speculative. All the experimental evidence discussed in this review has described heterogeneity in dynamics and not heterogeneity in structure. At present, there is no definitive evidence for the structural origin of these heterogeneities. Small-angle neutron and X-ray scattering studies have been performed in supercooled liquids in an effort to characterize any temperature-dependent structural heterogeneity. Leheny and coworkers (13) performed neutron scattering experiments on propylene glycol. With changing temperature, the only changes noted were in the large q range (corresponding to small changes in nearest-neighbor packing) and in the small q range (corresponding to changes in the compressibility of the liquids). They were able to show that the scattering data were not consistent with the existence of clusters in the range of 3–100 nm if the density difference between the clusters and the surrounding material was 5%. Fischer (90a) reported structural evidence for very interesting large clusters (roughly 100 nm) in several supercooled liquids. The origin of these large clusters is not completely understood, but because samples with and without these clusters show the same molecular motion near T_g , it seems clear that these large clusters are not directly responsible for heterogeneity in the α relaxation. The high-temperature computer simulations that show heterogeneous dynamics have also been analyzed in efforts to understand what makes slow particles slow. The candidates examined so far include local density, local packing symmetry, and potential energy (31, 32). In simulations of two-component systems, a correlation has been found between potential energy and mobility, but this was explained by small fluctuations in the local composition (32). Thus, even in this high-temperature regime, it is not clear what the structural signature of dynamic heterogeneity is for a single-component liquid. At present, it is an article of faith that something in the structure is responsible for dynamics that vary by orders of magnitude from one region of the sample to another at T_g . It is possible that efforts so far have failed because the structural signatures

are too subtle to be detected given experimental/statistical noise or because the wrong variables are being studied, e.g. we do not know a priori that local density correlates with local relaxation times.

The mode coupling theory (17, 18) that has attracted so much attention in regard to its prediction for high-temperature relaxation in supercooled liquids is not useful for addressing this question. The idealized version of the theory cannot be used in the vicinity of the laboratory T_g because it predicts a divergence of relaxation times at a considerably higher temperature. So far, extensions to the theory that might make it applicable at lower temperatures have not succeeded in reproducing the rich features obtained in experiments that have been attributed to spatial heterogeneity (91). In the temperature range above the predicted divergence, computer simulations show heterogeneity, as indicated by non-Gaussian van Hove functions. The magnitude of this non-Gaussian behavior substantially exceeds what is predicted by the mode coupling theory for a single component liquid. However, because the simulations are performed on a mixture of Lennard-Jones spheres of different sizes, this discrepancy may not reflect a failure of the mode coupling theory (92).

As described above, Kivelson et al (22) have a theory built upon the idea of frustration-limited domains, i.e. structures that are preferred in terms of free energy but cannot extend indefinitely because they do not fill space efficiently. Slow relaxation of the frustrated domains gives rise to slow relaxation in the supercooled liquids. If one associates the distribution of domain sizes with a distribution of relaxation times, then connections with the experimental observations of spatially heterogeneous dynamics are possible. Because of the mesoscopic nature of the theory, some fitting parameters are required to make these comparisons. Within this framework, the theory has been shown to be consistent with the temperature dependence of the relaxation of fragile supercooled liquids (22), and it also reasonably reproduces the distribution of relaxation times associated with molecular relaxation (93). Qualitatively correct behavior for the enhancement of translational diffusion has been calculated (93). A key aspect of this approach is that domain size determines local relaxation times at a given temperature. Although no experimental information is directly available on this point, it is an interesting target for experimental investigation.

The energy landscape picture has been increasingly utilized in discussions of the thermodynamic properties of supercooled liquids (20, 94). Unfortunately, connections between the energy landscape and the translational/rotational motion of molecules are not straightforward. For one model glass former, computer simulations show a correlation between position on the underlying landscape and particle mobility (89, 89a). Diezemann (58) produced a free energy landscape model that reproduces many of the features of the α relaxation, including the interesting differences between orientation relaxation measurements of order 1 and 2. Surprisingly, this model (95) succeeds in describing the enhancement of translational diffusion without explicitly invoking spatial heterogeneity, although it may implicitly account for such heterogeneity in its coarse-grained description of the free energy

landscape. In principle, this model could be checked against the nonexponential intermediate scattering functions described by Figure 11. This model suggests that the exchange process should not be viewed as a separate process but merely as another manifestation of the α relaxation. As such, it cannot explain the data in Figures 5 and 6 that show exchange times much longer than the average relaxation time. If these results have been correctly interpreted, modifications to the Diezemann model would be required to explain data very near T_g .

Xia & Wolynes (95a) have very recently extended the random first-order transition theory of glasses based on the apparent near universality of a Lindemann ratio describing the largest possible thermal motion consistent with a fixed local structure. Their calculation reproduces the experimental correlation between fragility and nonexponential relaxation and predicts that the size of heterogeneous regions is on the order of four molecular diameters for a fragile liquid. Other experimental observables associated with spatially heterogeneous dynamics have not yet been addressed within this theory.

Models built upon equilibrium fluctuations in the density and/or entropy naturally give rise to spatially heterogeneous dynamics (96, 97). It was recently shown that such a model can account qualitatively for the enhanced translational diffusion in three different glass formers (98). The basic idea of this model is easily expressed. For simplicity, here we consider only density fluctuations. Individual molecules are assumed to reorient with a characteristic time, which is controlled by the density in a small region surrounding the molecule (with a radius of perhaps 1–2 nm). Density fluctuations on these length scales can be reasonably predicted using macroscopic properties (such as the compressibility). The variation in relaxation times associated with density variations can be estimated from the change in the average relaxation time with overall system density. Within the context of this model, the increasing manifestations of spatially heterogeneous dynamics with decreasing temperature are easily explained. Density fluctuations on the relevant length scale are largely independent of temperature, but the influence of a density variation on the dynamics becomes much more important at lower temperatures. (This last point is qualitatively consistent with the simplest free volume model.) Within the context of this fluctuation model, there is no special structural length scale. This is consistent with existing scattering data. However, there is a special dynamical length scale that describes a “sphere of influence” that determines the relaxation properties of a given molecule. This model provides no insight into the extremely long exchange times that are shown in Figures 5 and 6 and is best viewed as a possible explanation for data more than a few degrees above the calorimetric T_g .

One experiment supports the view that local density is correlated with local mobility near T_g . The intensity of light scattering during temperature scans through the glass transition shows an interesting hysteresis (99). Moynihan & Schroeder (97) and Moynihan & Whang (100) have produced the only reasonable interpretation of this phenomenon to date argues that regions of different local density must be relaxing at different rates in order to produce the experimental effect. This

result does not demand that local density be the cause of spatial heterogeneity in dynamics, but it does suggest that if something else is responsible for spatial heterogeneity, this something else is also coupled to local density fluctuations. Candidates would include local configurational entropy (97, 98) and local orientational order.

The suggestions for the origin of the spatially heterogeneous dynamics fall into two categories. One class of explanations (density and/or configurational entropy fluctuations) views heterogeneity in dynamics as a secondary effect of slow dynamics. That is, no matter what mechanism is responsible for slow dynamics, one would expect these heterogeneities to result. The other set of explanations (frustration-limited domains, energy landscape model) views heterogeneity as an integral part of the mechanism for slow dynamics. If the second viewpoint is correct, then the experimental characterization of spatially heterogeneous dynamics provides what is arguably the richest source of information about the origin of slow dynamics near T_g .

CONCLUDING REMARKS

In spite of our tendency to think of liquids as homogeneous, deeply supercooled liquids are surprisingly heterogeneous in terms of their dynamics. Molecules only a few nanometers away from each other may have relaxation rates that differ by several orders of magnitude. In addition to being responsible for commonly observed nonexponential ensemble average relaxation processes, these spatially heterogeneous dynamics cause translational diffusion coefficients to be orders of magnitude larger than expected.

Spatial heterogeneity in dynamics qualitatively and quantitatively distinguishes dynamics near T_g from the behavior of liquids at high temperature. Thus although it has sometimes been argued that supercooled liquids can be completely understood by studying the dynamics of liquids in the nanosecond regime, I would claim that this is not the case. As one example, experiments and simulations on liquids with fast dynamics indicate that translational motion becomes Fickian by the time the average particle has moved about one diameter. In contrast, near T_g translational motion is non-Fickian even after the average particle has moved more than 100 diameters.

The ultimate significance of these spatial heterogeneities in the dynamics of supercooled liquids is not clear. Even if they are only a side show to the main event (slowing dynamics), they must be understood in order to predict transport and relaxation properties of glass-forming materials, as well as their crystallization behavior (99a). On the other hand, these dynamic heterogeneities might turn out to be our best handle on the cause of slow dynamics. The apparent sudden increase in the lifetimes of these regions very near T_g fits into this second scenario, and new experiments that clarify this issue are a high priority. Any significant increase in the length scale of heterogeneity in this temperature range would also argue

that spatial heterogeneities are at the heart of glass transition dynamics, at least for fragile glass formers. Given the similarities between glass formation and other systems with slow dynamics (e.g. protein folding and granular materials), the ramifications of a clearer understanding of the slow dynamics that lead to glass formation could be felt in a number of fields.

The influence of spatial heterogeneities in dynamics in the glassy state is almost unexplored (76, 97, 100–103). Intuition argues that they cannot cease to be significant just because T_g has been traversed. It might be expected that such heterogeneities would have a major influence on relaxation toward equilibrium from the nonequilibrium glassy state. This important problem is notoriously complex (5) but might be amenable to new approaches that account for spatial heterogeneities in dynamics.

ACKNOWLEDGMENTS

The research from my own laboratory described in this review has been funded by the National Science Foundation (Chemistry Division). I am indebted to current and former coworkers in my laboratory and, in particular, want to thank Forrest Blackburn, Marc Cicerone, and Chia-Ying Wang. Ideas from discussions with colleagues at other institutions are woven throughout this review, and I particularly acknowledge Austin Angell, Dan Kivelson, Walter Kob, Connie Moynihan, Sid Nagel, and Ranko Richert.

Visit the Annual Reviews home page at www.AnnualReviews.org

LITERATURE CITED

- Sillescu H. 1999. *J. Non-Cryst. Solids* 243:81–108
- Bohmer R. 1998. *Curr. Opin. Solid State Mat. Sci.* 3:378–85
- Ediger MD, Angell CA, Nagel SR. 1996. *J. Phys. Chem.* 100:13200–12
- Lunkenheimer P, Schneider U, Brand R, Loidl A. 2000. *Contemp. Phys.* 41:15–36
- McKenna GB. 1990. In *Comprehensive Polymer Science*, ed. C Booth, C Price, 2:311–62 Oxford, UK: Pergamon
- Angell CA. 1995. *Science* 267:1924–35
- Stillinger FH. 1995. *Science* 267:1935–39
- Tarjus G, Kivelson D. Submitted for publication
- Fredrickson GH. 1988. *Annu. Rev. Phys. Chem.* 39:149–80
- Debenedetti PG. 1996. *Metastable Liquids. Concepts and Principles*. Princeton, NJ: Princeton Univ. Washington Press
- Angell CA, Ngai KL, McKenna GB, McMillan PF, Martin SW. 2000 *J. Appl. Phys.* In press
- Angell CA. 1984. In *Relaxations in Complex Systems*, ed. KL Ngai, GB Wright, pp. 3–11. Naval Res. Lab.
- Chang I, Fujara F, Geil B, Heuberger G, Mangel T, Sillescu H. 1994. *J. Non-Cryst. Solids* 172/174:248–55
- Leheny RL, Menon N, Nagel SR, Price DL, Suzuya K, Thiyagarajan P. 1996. *J. Chem. Phys.* 105:7783–94
- Tolle A, Schober H, Wuttke J, Fujara F. 1997. *Phys. Rev.* E56:809–15
- Morineau D, Alba-Simionesco C, Bellissent-Funel MC, Lauthie MF. 1998. *Europhys. Lett.* 43:195–200
- Ferrer ML, Lawrence C, Demirjian BG,

- Kivelson D, Alba-Simionesco C, Tarjus G. 1998. *J. Chem. Phys.* 109:8010–15
17. Bengtzelius U, Goetze W, Sjolander A. 1984. *J. Phys. C* 17:5915
18. Leuthusser E. 1984. *Phys. Rev. A* 29: 2765
19. Adam G, Gibbs JH. 1965. *J. Chem. Phys.* 43:139–46
20. Angell CA. 1997 *J. Res. Natl. Inst. Stand. Technol.* 102:171–85
- 20a. Richert R, Angell CA. 1998. *J. Chem. Phys.* 108:9016–26
21. Ngai KL. 1999. *J. Phys. Chem. B* 103: 5895–902
22. Kivelson D, Kivelson SA, Zhao XL, Nussinov Z, Tarjus G. 1995. *Physica A* 219:27–38
23. Cicerone MT, Blackburn FR, Ediger MD. 1995. *Macromolecules* 28:8224–32
24. Plazek DJ. 1965. *J. Phys. Chem.* 69:3480–87
25. Ilan B, Loring RF. 1999. *Macromolecules* 32:949–51
26. Richert R, Heuer A. 1997. *Macromolecules* 30:4038–41
27. Shamblin SL, Tang XL, Chang LQ, Hancock BC, Pikal MJ. 1999. *J. Phys. Chem. B* 103:4113–21
28. Fox KC. 1995. *Science* 267:1922–23
29. Miller DP, Anderson RE, de Pablo JJ. 1998. *Pharm. Res.* 15:1215–21
30. Champion D, Hervet H, Blond G, LeMeste M, Simatos D. 1997. *J. Phys. Chem. B* 101:10674
31. Perera DN, Harrowell P. 1999. *J. Chem. Phys.* 111:5441–54
32. Donati C, Glotzer SC, Poole PH, Kob W, Plimpton SJ. 1999. *Phys. Rev. E* 60:3107–19
33. Yamamoto R, Onuki A. 1998. *Phys. Rev. Lett.* 81:4915–18
34. Johnson G, Mel'cuk A, Gould H, Klein W, Mountain RD. 1998. *Phys. Rev. E* 57:5707–18
35. Hurley MM, Harrowell P. 1995. *Phys. Rev. E* 52:1694–98
36. Donati C, Douglas JF, Kob W, Plimpton SJ, Poole PH, Glotzer SC. 1998. *Phys. Rev. Lett.* 80:2338–41
37. Schmidt-Rohr K, Spiess H. 1991. *Phys. Rev. Lett.* 66:3020
38. Cicerone MT, Ediger MD. 1995. *J. Chem. Phys.* 103:5684–92
39. Schiener B, Chamberlin RV, Diezemann G, Bohmer R. 1997. *J. Chem. Phys.* 107:7746–61
40. Bohmer R, Hinze G, Diezemann G, Geil B, Sillescu H. 1996. *Europhys. Lett.* 36:55–60
41. Hinze G, Diezemann G, Sillescu H. 1998. *Europhys. Lett.* 44:565–70
42. Hinze G. 1998. *Phys. Rev. E* 57:2010–18
43. Heuer A, Wilhelm M, Zimmermann H, Spiess H. 1995. *Phys. Rev. Lett.* 75:2851
44. Kuebler SC, Heuer A, Spiess HW. 1997. *Phys. Rev. E.* 56:741
45. Cicerone MT, Ediger MD. 1993. *J. Phys. Chem.* 97:10489–97
46. Cicerone MT, Ediger MD. 1996. *J. Chem. Phys.* 104:7210–18
47. Wang CY, Ediger MD. 1999. *J. Phys. Chem. B* 103:4177–84
48. Wang CY, Ediger MD. 2000. *J. Chem. Phys.* In press
- 48a. Cugliandolo LF, Iguain JL. Submitted for publication
49. Russell EV, Israeloff NE, Walther LE, Gomariz HA. 1998. *Phys. Rev. Lett.* 81:1461–64
50. Ha T, Laurence TA, Chemla DS, Weiss S. 1999. *J. Phys. Chem. B* 103:6839–50
51. Bartko AP, Dickson RM. 1999. *J. Phys. Chem. B* 103:11237–41
52. Ishikawa M, Ye JY, Maruyama Y, Nakatsuka H. 1999. *J. Phys. Chem. A* 103:4319–31
53. Richert R. 1992. *Chem. Phys. Lett.* 199:355–59
54. Richert R, Stickel F, Fee RS, Maroncelli M. 1994. *Chem. Phys. Lett.* 229:302–8
55. Richert R. 1994. In *Disorder Effects on*

- Relaxational Processes*, ed. R Richert, A Blumen, pp. 333–58, Berlin: Springer
56. Richert R. 1997. *J. Phys. Chem. B* 101:6323
57. Wendt H, Richert R. 2000. *Phys. Rev. E*. In press
58. Diezemann G. 1997. *J. Chem. Phys.* 107:10112–20
59. Donth E. 1982. *J. Non-Cryst. Solids* 53:325–30
60. Rizos AK, Ngai KL. 1999. *Phys. Rev. E* 59:612–17
61. Yamamuro O, Tsukushi I, Lindqvist A, Takahara S, Ishikawa M, Matsuo T. 1998. *J. Phys. Chem. B* 102:1605–9
62. Cicerone MT, Blackburn FR, Ediger MD. 1995. *J. Chem. Phys.* 102:471–79
63. Barut G, Pissis P, Pelster R, Nimtz G. 1998. *Phys. Rev. Lett.* 80:3543–56
64. Huwe A, Kremer F, Behrens P, Schwieger W. 1999. *Phys. Rev. Lett.* 82:2338
65. Keddie JL, Jones RAL, Cory RA. 1994. *Europhys. Lett.* 27:59–64
66. Tracht U, Wilhelm M, Heuer A, Spiess HW. 1999. *J. Magn. Reson.* 140:460–70
67. Fujara F, Geil B, Sillescu H, Fleischer G. 1992. *Z. Phys. B* 88:195
68. Tarjus G, Kivelson D. 1995. *J. Chem. Phys.* 103:3071–73
69. Stillinger FH, Hodgdon JA. 1994. *Phys. Rev. E* 50:2064–68
- 69a. Cicerone MT. 1994. PhD thesis. Univ. Wisconsin-Madison.
70. Qian J, Hentschke R, Heuer A. 1999. *J. Chem. Phys.* 110:4514–22
71. Davis HT. 1977. *J. Am. Ceram. Soc.* 60:499
72. Zwanzig R. 1989. *Chem. Phys. Lett.* 164:639
73. Cicerone MT, Wagner PA, Ediger MD. 1997. *J. Phys. Chem. B* 101:8727–34
74. Perera DN, Harrowell P. 1998. *Phys. Rev. Lett.* 81:120–23
75. Bainbridge D, Ediger MD. 1997. *Rheol. Acta* 36:209–16
76. Hall DB, Dhinojwala A, Torkelson JM. 1997. *Phys. Rev. Lett.* 79:103–6
77. Wang CY, Ediger MD. 2000. *J. Phys. Chem. B* In press
78. Kob W, Andersen HC. 1995. *Phys. Rev. E* 51:4626–41
79. Wuttke J, Chang I, Randl OG, Fujara F, Petry W. 1996. *Phys. Rev. E* 54:5364–69
- 79a. Ngai KL. 1999. *J. Phys. Chem. B* 103:10684–94
80. Bohmer R, Chamberlin RV, Diezemann G, Geil B, Heuer A, et al. 1998. *J. Non-Cryst. Solids* 235:1–9
81. Bohmer R, Ngai KL, Angell CA, Plazek DJ. 1993. *J. Chem. Phys.* 99:4201
82. Wang CY, Ediger MD. 1997. *Macromolecules* 30:4770–71
83. Blackburn FR, Wang CY, Ediger MD. 1996. *J. Phys. Chem.* 100:18249–57
84. Hinze G, Sillescu H. 1996. *J. Chem. Phys.* 104:314–19
85. Chang I, Sillescu H. 1997. *J. Phys. Chem. B* 101:8794–801
86. Heuberger G, Sillescu H. 1996. *J. Phys. Chem.* 100:15255–60
87. Goldstein M. 1969. *J. Chem. Phys.* 51:3728
88. Angell CA. 1988. *J. Phys. Chem. Solids* 49:863
89. Sastry S, Debenedetti PG, Stillinger FH. 1998. *Nature* 393:554–57
- 89a. Buchner S, Heuer A. Submitted for publication
90. Smith RS, Kay BD. 1999. *Nature* 398:788–91
- 90a. Fischer EW. 1993. *Physica A* 201:183–206
91. Bhattacharyya S, Bagchi B. 1997. *J. Chem. Phys.* 107:5852–62
92. Fuchs M, Gotze W, Mayr MR. 1998. *Phys. Rev. E* 58:3384–99
93. Tarjus G, Kivelson D, Kivelson S. 1996. *Supercooled Liquids, Advances and Novel Applications, ACS Symp. Ser.* 676, pp. 67–81. Washington, DC: Am. Chem. Soc.
94. Sciortino F, Kob W, Tartaglia P. 1999. *Phys. Rev. Lett.* 83:3214–17
95. Diezemann G, Sillescu H, Hinze G,

- Bohmer R. 1998. *Phys. Rev. E* 57:4398–410
- 95a. Xia X, Wolynes PG. 2000. *Proc. Natl. Acad. Sci. USA*. In press
96. Robertson RE. 1978. *J. Polym. Sci. Polym. Symp.* 63:173
97. Moynihan CT, Schroeder JJ. 1993. *J. Non-Cryst. Solids* 160:52–59
98. Ediger MD. 1998. *J. Non-Cryst. Solids* 235/237:10–18
99. Bokov NA, Andreev NS. 1989. *Sov. J. Glass Phys. Chem.* 15:243
- 99a. Harrowell P, Oxtoby DW. 1993. *Ceramic Trans.* 30:35–44
100. Moynihan CT, Whang JH. 1997. *Mater. Res. Soc. Symp. Proc.* 455:133–39
101. Hwang Y, Inoue T, Wanger PA, Ediger MD. 2000. *J. Polym. Sci. B Polym. Phys.* 38:68–79
102. Miller RS, MacPhail RA. 1997. *J. Phys. Chem. B* 101:8635–41
103. Bohmer R, Hinze G, Jorg T, Qi F, Sillescu H. 2000. *J. Phys. Condens. Matter*. In press